Macroscopic contraction of a gel induced by the integrated motion of light-driven molecular motors

Quan Li, Gad Fuks, Emilie Moulin, Mounir Maaloum, Michel Rawiso, Igor Kulic, Justin Foy, Nicolas Giuseppone

Macroscopic contraction of a gel induced by the integrated motion of light-driven molecular motors

Quan Li,[1,2] Gad Fuks,[1,2] Emilie Moulin,[1,2] Mounir Maaloum,[1,2] Michel Rawiso,[2] Igor Kulic,[2] Justin T. Foy,[1,2] and Nicolas Giuseppone[1,2]*

[1] SAMS research group

[2] Institut Charles Sadron, University of Strasbourg – CNRS

23 rue du Loess, BP 84047, 67034 Strasbourg Cedex 2, France

*e-mail: giuseppone@unistra.fr

Making molecular machines that can be useful in the macroscopic world is a challenging long-term goal of nanoscience.[1] Inspired by the protein machinery found in biological systems,[2,3] and based on the theoretical understanding of the physics of motion at the nanoscale,[4,5] organic chemists have developed a number of molecules that can produce work by contraction or rotation when triggered by various external chemical or physical stimuli.[6,7,8,9] In particular, basic molecular switches that commute between at least two thermodynamic minima, and more advanced molecular motors that behave as dissipative units working far from equilibrium when fuelled with external energy[10,11,12,13] have been reported. However, despite recent progresses,[14,15,16,17] the ultimate challenge to coordinate individual molecular motors in a continuous mechanical process that can have a measurable effect at the macroscale has remained elusive.[18,19] Here we show that by integrating light-driven unidirectional molecular rotors as reticulating units in a polymer gel, it is possible to amplify their individual motions to achieve macroscopic contraction of the material. Our system uses the incoming light to operate under far-from-equilibrium conditions and the work produced by the motor in the photostationary state is used to twist the entangled polymer chains up to the collapse of the gel. Our design could be a starting point to integrate nanomotors in metastable materials to store energy and eventually to convert it.

The active chemical structures used in this study involve modifications of rotary motor **1** (Fig. 1). This functional core unit takes inspiration from the seminal work of Feringa and collaborators and, in particular, from their development of a second generation of light-driven motors which can rotate with high frequencies (up to 3 MHz).[20,21,22] For further incorporation in responsive macroscopic materials, we have first developed an original asymmetric synthetic pathway which allows for the gram-scale synthesis of enantiopure functional motors (see Supplementary Information for the synthesis and characterization of the molecules). By introducing two chiral auxiliaries of (*R*) configuration, the stereochemistry of (*R*,*R*,*S*)-**1** can be fully assigned thanks to single-crystal X-ray diffraction. Such chiral motors produce unidirectional rotation when pushed far from equilibrium by continuously repeating a sequence of light-activated *cis-trans* isomerization of the central double-bond combined with a thermal helix inversion.[13] In addition, **1** was modified with two orthogonal sets of two protected reactive groups in its upper and bottom parts (ethyl esters and *tert*-butyldimethylsilyl ethers, respectively) in order to connect it further with polymer chains and to enforce entanglement upon rotation. Following a series of chemical transformations, compounds **2** and **3** were obtained as key polymer-motor conjugates. Even though both of them incorporate two chains of tri(ethylene glycol) with a terminal alkyne in their bottom part, they differ from the molecular weight of the azide-terminated poly(ethylene glycol) attached to their upper part (M = 5 000 g.mol^{-1} for **2**, and M = 10 000 g.mol^{-1} for **3**). In this orthogonal configuration, and at high dilution, the two bottom alkyne groups of a single polymer-motor conjugate can selectively react with its two upper azides by a copper-catalysed Huisgen[3+2] cycloaddition ("click reaction"), which leads to

the formation of two triazole units. This double intramolecular cyclisation is very efficient to produce with good yields 8-shaped polymers **4** and **5** containing the rotary motor in their centers. By using the same click reaction, but at higher concentration, the subsequent intermolecular formation of triazoles leads to cross-linked chemical gels **6** and **7** which incorporate the rotary motors as reticulation units.

The 8-shaped configuration is considered complementary to the gel for probing the effect of light-induced rotation in a discrete self-entangled macromolecule (Fig. 2). In particular, we have performed small angle X-ray scattering (SAXS) on both compounds **4** and **5** in dilute toluene solutions. By using a Kratky representation of the scattered intensity, we can observe the presence of a characteristic bump for a figure-of-eight polymer,[23] with a radius of gyration (R_g) associated to the position of the peak in the reciprocal space (R_g(**4**) = 2.58 nm; R_g(**5**) = 3.48 nm). These values are in agreement with theory for 8-shaped polymers made of polyethylene glycol and having such molecular weights (see Supplementary Information for details). Interestingly, when compound **4** is irradiated in toluene with a UV lamp of 6W (0.96 mW.cm^{-2} at 366 nm), the shifts of the scattering peaks in the Kratky plot indicate an evolution towards smaller radius of gyration values (from 2.58 nm to 2.24 nm). In addition, the 50% increase of the scattered intensity reveals much higher internal densities of the polymer. This global behavior is expected for a mechanically enforced coiling of the self-entangled polymer chains upon rotation of the motor. These results, obtained on an average population of 8-shaped polymers in the reciprocal space, are confirmed by imaging individual macromolecules **5** in the real space thanks to

atomic force microscopy (AFM) using the peak force tapping mode. In its initial state, the 8-shape is clearly evidenced when unfolded on a mica surface. The diameter of each ring is in the range of 15 nm, which is in good agreement with the expected theoretical value for a cyclic 10 000 PEG chain (Supplemntary Information). After UV light irradiation for 15 min, no more 8-shaped configurations are detected by AFM, but only collapsed (spherical or more elongated) coils with smaller dimensions. This type of conformation is expected regarding the winded topology of the contracted 8 upon rotation of the motor.

For chemically cross-linked polymer-motor conjugates in the form of gel **6** at 10% w/w in toluene, fluorescence and macroscopic contractions are satisfyingly observed at room temperature thanks to a simple irradiation with UV light (Fig. 3 and Supplementary Movie 1). We concomitantly performed a control experiment for which a similar gel was synthesized, but having the rotating double bond blocked by an episulfide function (see compound **28** in Scheme S7). In this case, the gel did not show any fluorescence and/or contraction after 240 min of irradiation in the same conditions, correlating the macroscopic contraction to the molecular rotation (Supplementary Movie 2). The macroscopic shape of the active gel **6** is not significantly modified during the contraction, indicating an isotropic process. By measuring the surface reduction of the gel after 120 min and assuming an isotropic effect on the volume, we approximate a maximum contraction of about 80%. After longer times of irradiation, we notice a rupture of this gel which recovers its initial volume and shape. This event is concomitant with the loss of fluorescence in the broken regions (see differences between z_1 (not yet broken) and z_2 (broken) in Fig. 3c, t = 170 min), indicating a probable disruption by oxidation of the motor double bond and a loss of conjugation, while keeping a

single bond and thus a reticulated topology when unwinded up to its initial swollen equilibrium state. The oxidative degradation of the double bond to a single one was supported by experiments on individual motors which can be damaged with long time UV irradiation and in the presence of air. This reactivity of the double bond is greatly enhanced when the gel becomes tensed, but it can be delayed for several hours by working under argon or by stopping the irradiation. In some experiments, the free energy contained in the tensed gel is so high and the dissipative rupture so sudden that it leads to a jump of the entire piece of gel in the vial (Supplementary Movie 3). The maximum of energy stored in the gel corresponds to the transfer in twisted entanglements of the free energy of the motor $\Delta G°$ (32 $kJ.mol^{-1}$; 12.8 k_BT per motor) and which characterizes the difference between its unstable thermal state and its stable thermal state during the helix inversion (Fig. 3d, red curve). Considering that the maximum of mechanical work stored in the gel requires 120 min of irradiation, and knowing the absorption of the gel at 366 nm over this period, one can estimate an energy conversion of 0.15% for the contraction (see Supplementary Information). To understand the correlations existing at all scales, we started by plotting the contraction of active gel **6** as a function of time (Fig. 3e). One can see that after an activation period comprised between 0 and 30 min, and corresponding to the time necessary to tense the polymer chains with the first twists, the contraction then enters an apparent linear regime for 60 min. This non-equilibrium steady state part of the contraction indicates that a single process of twisting is involved (and that is not followed by a supercoiling of the polymer chains which would produce a second regime of contraction). Then, the contraction slows down at higher tension and all the double bond breaks simultaneously at the maximum of twisted

torsion, representing an interesting type of chemical activation upon mechanical constraints. One can estimate the maximum number of turn ($n < 105$) in the twisted configuration during this time of contraction, as being the ratio between the contour length (L_c) of the PEG 5 000 polymer (that is 40 nm) and its persistence length (L_p, that is 0.38 nm). It results that the maximum frequency for the motor in the gel is $F_{gel\mathbf{6}} = 3.16\ 10^{-2}$ Hz ($t_{1/2gel\mathbf{6}} = 22$ seconds) at 25°C, corresponding to an activation energy $\Delta G^{\neq}_{gel\mathbf{6}} = 81.5$ kJ.mol^{-1} (as the rate limiting step of the process is the thermal helix inversion).[24,25] This can be compared with the activation energy for the polymer free motor determined by DFT calculations ($\Delta G^{\neq}_{free} = 31.9$ kJ.mol^{-1}; $F_{free} = 8.05$ MHz; $t_{1/2free} = 4.3\ 10^{-8}$ s at 25°C), and which is in good agreement with similar structures in the literature.[25,26] This extra 50 kJ.mol^{-1} for gel **6** represents the penalty to twist the reticulated polymer chains, also meaning that the slope of the contraction as a function of time should be dependent on the size[27] of the polymers linking the dissipative units of the gel. As an example, by contracting gel **7** (with PEG chains having a double molecular weight of 10 000 g.mol^{-1}), we could not visualize significant contraction at room temperature after 8 hours. However, by raising the temperature to 50°C, a maximum contraction was evidenced after 18 hours, illustrating a slower rotation frequency of $F_{gel\mathbf{7}} = 3.28\ 10^{-3}$ Hz ($t_{1/2gel\mathbf{7}} = 105$ s) at 50°C, giving $\Delta G^{\neq}_{gel\mathbf{7}} = 87.0$ kJ.mol^{-1}, and which after extrapolation at 25°C ($1.74\ 10^{-3}$ Hz; $t_{1/2} = 200$ s) gives a speed one order of magnitude slower than **6**. Interestingly, gel **7** also leads to a maximum contraction of 75-80% (Supplementary Movie 4). By looking closer at the topological process, one can determine that in principle the maximum contraction is reached for any polymer when each twist reaches the most tensed circular curvature with a minimum radius related to L_p. As L_c is invariant, the size

of such a twisted chain compared to its untwisted form was determined to be 66% (25% in volume). This simple model also indicates that (*i*) n_{max} should be dependent on L_p for each given polymer, and that (*ii*) for sufficiently soft twisted polymer chains and without supercoiling, the contraction should be always close to a ratio of $(2/\pi)^3$ for the maximum number of turn (n_{max}) at the end of the process, as observed experimentally (see Supplementary Information).

This very strong macroscopic contraction was also probed at the microscopic scale by AFM (Fig. 4). Images of the gel surface show an important change in the average size of the pore diameters when comparing the initial state (8 nm) and the contracted state (20 nm). This confirms that the macroscopic contraction is the result of the microscopic twisting of entangled polymer chains in the tensed gel, leaving more empty spaces (i.e. larger pores) between denser winded regions. The initial size of the pores is recovered after oxidation of the motor double bond to a single one for longer times of irradiation, which is also in agreement with an uncoiling of the gel while keeping its overall network topology. Complementary SAXS experiments show that the Lorentzian analytical form prevailing for a semi-dilute polymer solution[28] cannot really describe the scattered intensity from gel **6** at swelling equilibrium. That presumably results from the existence of heterogeneities as well as from the form factor of the chemical junctions in the gel. Nevertheless, we measure a very strong increase of the scattered intensity upon irradiation, indicating a densification of the polymer chains by aggregation and shrinkage at maximum contraction, in agreement with macroscopic and AFM observations as well as with the proposed simplified model of twisting.

The unidirectional rotations of molecular motors fuelled by light and working out of equilibrium are thus able to produce powerful macroscopic contraction by

operating together in a fully integrated metastable system when coupled to properly entangled polymer chains. This actuation results from the work performed by the motor that twists the polymer chains (instead of being fully dissipated thermally), and transforms a nanorotation into a contraction event at higher scales. In such a topology, the maximum number of turns n_{max} is dependant on L_p and L_c, but the contraction ratio is invariant when reaching n_{max}. The rate of rotation in the gel is strongly dependent on the size of the polymer but, with a suitable chemical design, it can reach sufficient frequencies at room temperature to be of practical interest. Such system represents a new and general way to connect molecular motors at all scales and up to the macroscopic one. By essence, it profoundly differs from any material based on machines that switch stepwise by a dual activation between two thermodynamic minima and which can work only when pre-oriented in the solid state[29,30] or at surfaces.[16,17] Indeed, our system can function: (*i*) continuously out of equilibrium, (*ii*) using a single stimulus, (*iii*) in an isotropic medium submitted to Brownian motion,[7] and (*iv*) by increasing its global free energy over time. In particular, this means that such materials can store energy from light in entangled polymer chains by mainly decreasing their entropy in twisted topologies. Further uses of this energy in other processes different from mechanical motions, such as in catalysis, represent some of the next possible challenges.

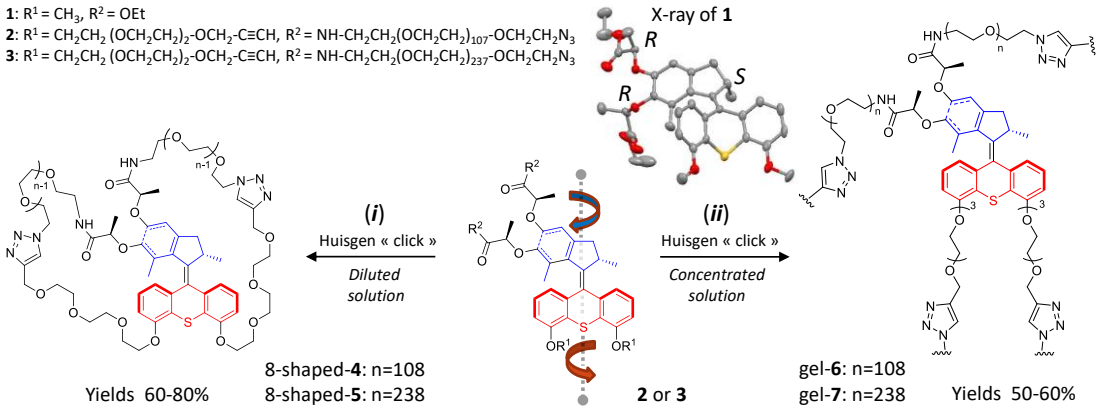

Figure 1 | General chemical design to access enantiopure polymer-motor conjugates. Key molecular motor intermediates **2** or **3** can be engaged either (***i***) in a double intramolecular "click" cyclisation catalysed by Cu(I) yielding 8-shaped compounds **4** and **5** which incorporate the rotary unit in their core; or (***ii***) in a intermolecular "click" cross-linkage catalysed by Cu(I) to yield chemical gels **6** and **7** which incorporate rotary units as mechanically active reticulating nodes. The blue color highlights the rotor part of the motor, while the red part shows the stator part, both linked by the axial photoisomerizable double bond.

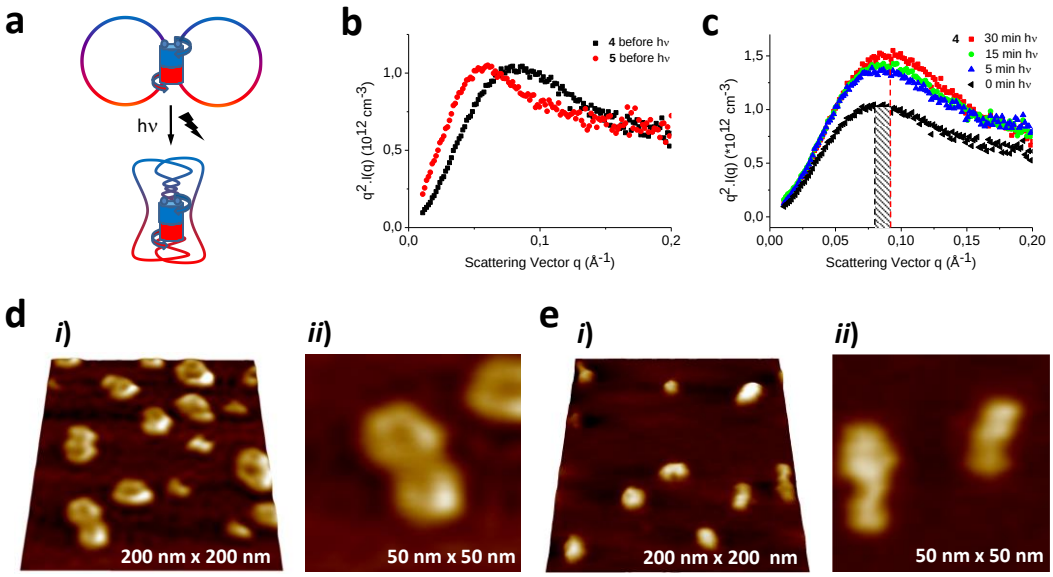

Figure 2 | Characterisation of mechanically active 8-shaped polymer-motor conjugates. **a,** Schematic representation of an 8-shaped polymer-motor conjugate which, due to its self-entangled topology, coils up the rings and reduces its size upon light-activated rotation. **b,** Kratky plot representation of the scattered intensities of 8-shaped compounds **4** and **5** ([c] = 10^{-2} g.cm^{-3} in toluene) before light irradiation. **c,** Kratky plot representation of the scattered intensities of 8-shaped compound **4** upon light irradiation; the dashed region shows the shift of the bump in the reciprocal space. **d,** AFM images of isolated uncoiled 8-shaped **5** on a mica surface before light irradiation. **e,** AFM images of isolated coiled 8-shaped **5** on a mica surface after 15 min of light irradiation (with a lamp power of 0.96 mW.cm^{-2}).

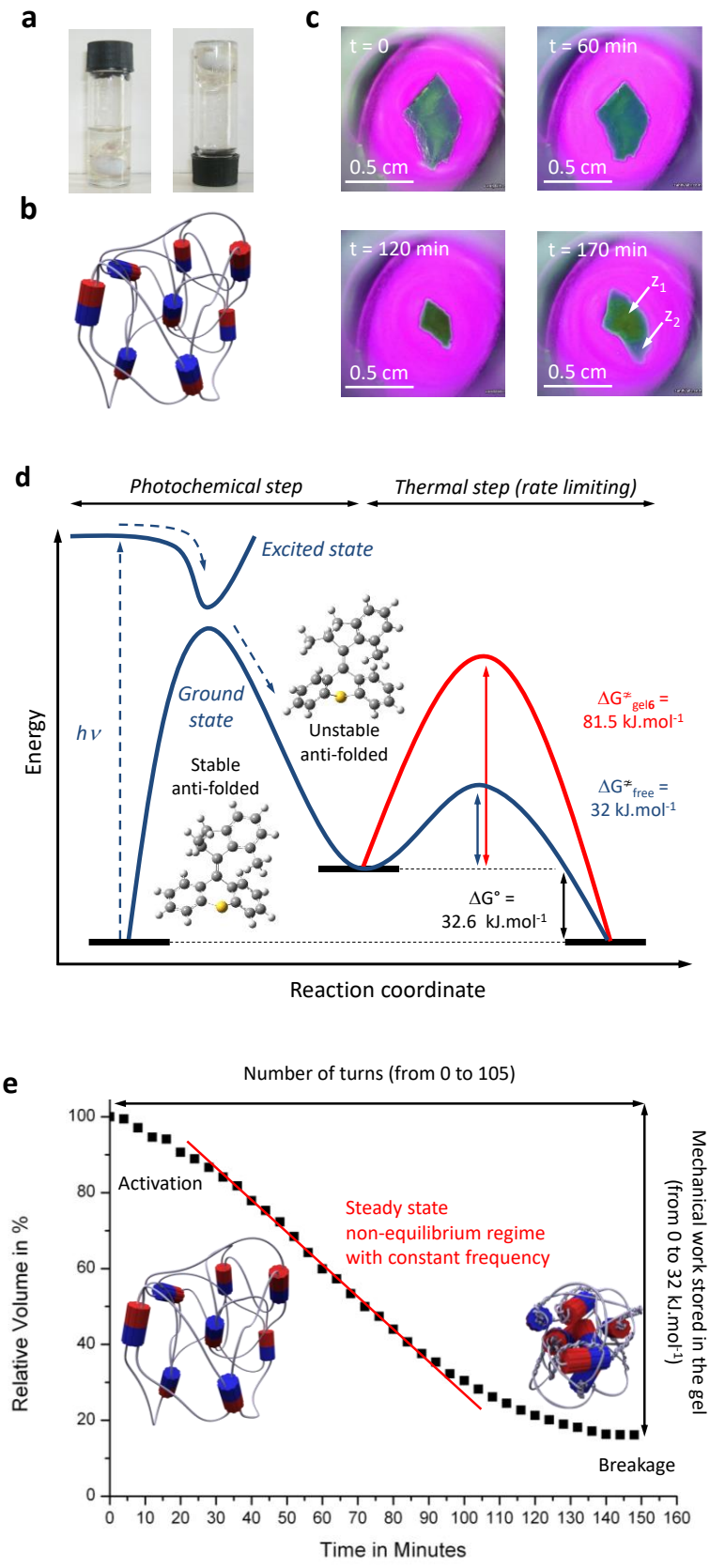

Figure 3 | Macroscopic behaviour of a mechanically active gel based on a chemically cross-linked polymer-motor conjugate system. a, Gel **6** at 10% w/w in toluene. **b,**

Schematic representation of a cross-linked polymer-motor conjugate which, due to its mechanically active entangled topology, coils up the polymer chains and reduces the entire size of the network upon light-activated rotation (see Fig. 3e). **c,** Snapshots taken from a movie (see Supplementary Information) showing time-dependent macroscopic contraction of a piece of gel **6** immersed in toluene and upon UV light irradiation (lamp power = 0.96 $mW.cm^{-2}$). At t = 170 min, z_1 corresponds to a region still contracted and z_2 corresponds to a region which starts disrupting. The gel is at the bottom of the vial and kept immersed in a large excess of toluene all along the experiment in order to keep it swollen in solvent and thus avoiding shrinkage by evaporation. **d,** Simplified energy diagram of the polymer free motor (blue) and of the polymer motor conjugate **6** (red) showing the typical variation of free energies for a 180° rotation and, in particular, highlighting the increase of the transition state in the gel by 50 $kJ.mol^{-1}$ during the rate limiting thermal step (helix inversion). The molecular models were obtained by DFT calculations. **e,** Overview of the contraction during the irradiation experiment, extracted from Supplementary movie 1, and showing the non-equilibrium steady state during the twisting of the polymer chains in an apparent linearity (red line is shown to guide the eye).

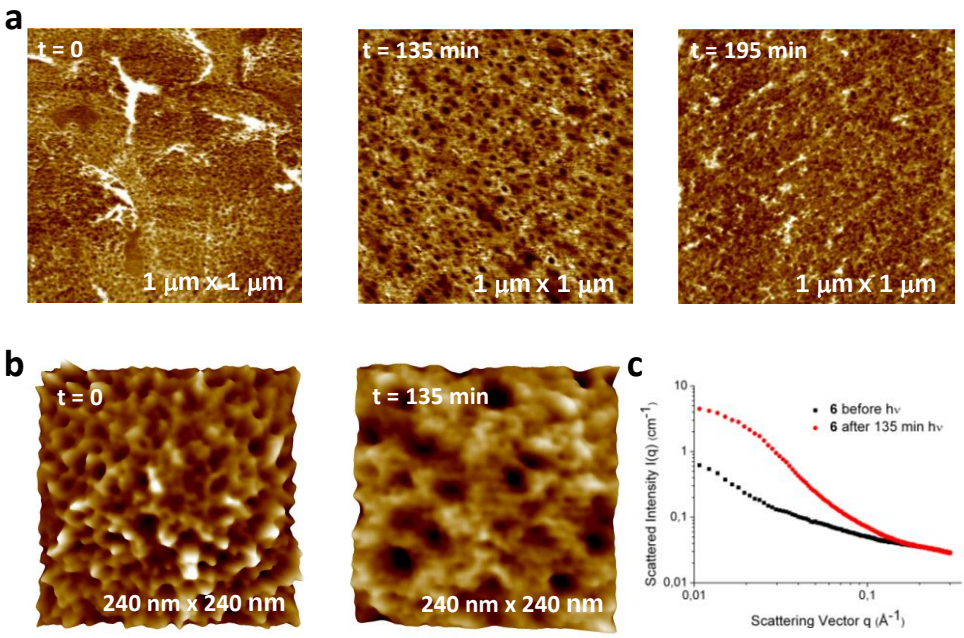

Figure 4 | Micro- and nanoscopic characterizations of mechanically active gels based on chemically cross-linked polymer-motor conjugates. a, AFM images of gel **6** submitted to different irradiation times of UV light (0.96 mW.cm^{-2}): before contraction (t = 0), after contraction (t = 135 min), and after rupture (t = 195 min). **b,** Detailed AFM images before and after contraction of gel **6** upon UV light irradiation, showing an increase of the average pore sizes from 8 nm to 20 nm. **c,** SAXS data obtained before and after irradiation of gel **6**.

Acknowledgements

The research leading to these results has received funding from the European Research Council under the European Community's Seventh Framework Program (FP7/2007-2013) / ERC Starting Grant agreement n°257099 (N.G.). We thank ANR (project INTEGRATIONS) for financial support. We also wish to thank the Centre National de la Recherche Scientifique (CNRS), the COST action (CM 1304), the international center for Frontier Research in Chemistry (icFRC), the Laboratory of Excellence for Complex System Chemistry (LabEx CSC), the University of Strasbourg (UdS), and the Institut Universitaire de France (IUF). Q.L. thanks the China Scholarship Council (CSC) for a doctoral fellowship. We thank Albert Johner for fruitful discussions. We also thank Mélodie Archimbaud for HPLC purifications, Guillaume Fleith for SAXS experiments, as well as Ran Liu and Tom Ellis for technical helps at various stages.

Author Contributions

N.G. directed the work. G.F., E.M., I.K., and N.G. conceived the work. Q.L., G.F., E.M., and N.G. designed the synthesis. Q.L. and J.F. performed the synthesis and Q.L. performed main chemical analyses and contraction experiments. M.M. performed the AFM imaging. M.R. performed and analyzed the X-ray scattering experiments. L.Q., M.R., and N.G. developed the contraction model. N.G. wrote the paper with all authors commenting on the manuscript.

Additional Information

Supplementary information accompanies this paper at www.nature.com/naturenanotechnology. Reprints and permission information is available online at http://npg.nature.com/reprintsandpermissions/. Correspondence and requests for materials should be addressed to N.G.

Competing Financial Interests

The authors declare no competing financial interests.

References

1. Feynman, R. “There’s plenty of room at the bottom.” *Caltech Engineering and Science* **23**, 22-36 (1960).
2. Schliwa, M. & Woehlke, G. Molecular motors. *Nature* **422**, 759-765 (2003).
3. Vale, R. D. & Milligan, R. A. The way things move : looking under the hood of molecular motor proteins. *Science* **288**, 88-95 (2000).
4. Jülicher, F., Ajdari, A. & Prost, J. Modeling molecular motors. *Rev. Mod. Phys.* **69**, 1269-1281 (1997).
5. Astumian, R. D. Thermodynamic and kinetics of a Brownian motor. *Science* **276**, 917-922 (1997).
6. Guix, M., Mayorga-Martinez, C. C. & Merkoçi, A. Nano/micromotors in (bio)chemical science applications. *Chem. Rev.* **114**, 6285-6322 (2014).
7. Coskun, A., Banaszak, M., Astumian, R. D., Stoddart, J. F. & Grzybowski, B. A. Great expectations: can artificial molecular machines deliver on their promise? *Chem. Soc. Rev.* **41**, 19-30 (2012).
8. Kay, E. R., Leigh, D. A. & Zerbetto, F. Synthetic molecular motors and mechanical machines. *Angew. Chem. Int. Ed.* **46**, 72-191 (2007).
9. Seeman, N. C. DNA in a material world. *Nature* **421**, 427-431 (2003).
10. Reinmann, P. Brownian motors: noisy transport far from equilibrium. *Phys. Rep.* **361**, 57-265 (2002).
11. Li, H. *et al.* Relative unidirectional translation in an artificial molecular assembly fueled by light. *J. Am. Chem. Soc.* **135**, 18609-18620 (2013).
12. Balzani, V. *et al.* Autonomous artificial nanomotor powered by sunlight. *Proc. Natl. Acad. Sci. USA.* **103**, 1178-1183 (2006).

13. Koumura, N., Zijlstra, R. W., van Delden, R. A., Harada, N. & Feringa, B. L. Light-driven monodirectional molecular motor. *Nature* **401**, 152-155 (1999).

14. Du, G., Moulin, E., Jouault, N., Buhler, E. & Giuseppone, N. Muscle‐like supramolecular polymers: integrated motion from thousands of molecular machines. *Angew. Chem. Int. Ed.* **51**, 12504-12508 (2012).

15. Eelkema, R. *et al.* Molecular machines: nanomotor rotates microscale objects. *Nature* **440**, 163 (2006).

16. Bernà, T. J. *et al.* Macroscopic transport by synthetic molecular machines. *Nature Mat.* **4**, 704-710 (2005).

17. Huang, J. *et al.* A nanomechanical device based on linear molecular motors. *Appl. Phys. Lett.* **85**, 5391-5393 (2004).

18. Browne, W. R. & Feringa, B. L. Making molecular machines work. *Nature Nanotech.* **1**, 25-35 (2006).

19. Feringa, B. L. & Browne, W. R. Macromolecules flex their muscles. *Nature Nanotech*. **3**, 383-384 (2008).

20. Klok, M. *et al.* MHz unidirectional rotation of molecular rotary motors. *J. Am. Chem. Soc.* **130**, 10484-10485 (2008).

21. London, G. *et al.* Light-driven altitudinal molecular motors on surfaces. *Chem. Commun.* 1712-1714 (2009).

22 Pollard, M. M. *et al.* Light-driven rotary molecular motors on gold nanoparticles. *Chem. Eur. J.* **14**, 11610-11622 (2008).

23. Shimamura, M. K., Kamata, K., Yao, A. & Degushi, T. Scattering functions of knotted ring polymers. *Phys. Rev. E* **72**, 041804 (2005).

24. Klok, M. *et al.* New mechanistic insight in the thermal helix inversion of second generation molecular motors. *Chem. Eur. J.* **14**, 11183-11193 (2008).

25. Cnossen, A., Kistemaker, J. C. M., Kojima, T. & Feringa, B. L. Structural dynamics of overcrowded alkene-based molecular motors during thermal isomerization. *J. Org. Chem*. **79**, 927-935 (2014).

26. Klok, M. Motors for use in molecular nanotechnology, PhD thesis, ISBN (digital version) 978-90-367-3706-7, University of Groningen (2009).

27. Chen, J., Kistemaker, J. C. M., Robertus, J. & Feringa, B. L. Molecular stirrers in action. *J. Am. Chem. Soc*. **136**, 14924-14932 (2014).

28. De Gennes, P.-G. Scaling concepts in polymer physics, Cornell University Press, New York (1979).

29. Yamada, M. *et al.* Photomobile polymer materials: towards light-driven plastic motors. *Angew. Chem. Int. Ed.* **47**, 4986-4988 (2008).

30. Ube, U. & Ikeda, T. Photomobile polymer materials with crosslinked liquid-crystalline structures: molecular design, fabrication, and function. *Angew. Chem. Int. Ed.* **53**, 10290-10299 (2014).